EXTERNAL RMP EFFECT ON LOCKED-MODE-LIKE INSTABILITY IN HELICAL PLASMAS

Y. TAKEMURA[1,2], K.Y. WATANABE[1,3], S. SAKAKIBARA[1,2], S. OHDACHI[1,4], Y. NARUSHIMA[1,2], K. IDA[1,2], M. YOSHINUMA[1,2] and LHD EXPERIMENT GROUP

[1] National Institute for Fusion Science, National Institutes of Natural Science, Toki, Gifu 509-5292, Japan
[2] The Graduate University for Advanced Studies, SOKENDAI, Toki, Gifu 509-5292, Japan
[3] Nagoya University, Graduate School of Engineering, Chikusa, Nagoya 464-8603, Japan
[4] The University of Tokyo, Graduate School of Frontier Sciences, Kashiwa, Chiba 277-8561, Japan

E-mail: takemura.yuki@nifs.ac.jp

Abstract

The slowing-down mechanism of the locked-mode-like instabilities with and without the island structure is investigated through the effects of an external RMP (Resonant Magnetic Perturbation) on the instabilities. For both instabilities, the slowing-down duration time decreases with the increase of the external RMP, and the RMP dependence is consistent with the braking model by the $\boldsymbol{j} \times \boldsymbol{B}$ force due to the interaction between the instabilities and the external RMP. Moreover, the relationship between the amplitude and the frequency of both locked-mode-like instabilities during the slowing-down is consistent with the force balance model between the $\boldsymbol{j} \times \boldsymbol{B}$ force due to the external RMP and a viscous force. These results suggest that the slowing-down of both locked-mode-like instabilities with the finite external RMP occurs due to the $\boldsymbol{j} \times \boldsymbol{B}$ force driven by the external RMP.

Keywords: MHD instability, rotation, RMP, helical plasma, LHD

1. Introduction

In the LHD (Large Helical Device), a reactor-relevant plasma with a volume-averaged beta value of 5 % can be stably maintained for more than ten times as long as the confinement time [1]. On the other hand, collapse events due to various MHD instabilities observed in different operational regimes cause serious degradation of confinement property: the torus-outward magnetic axis shift configuration ($R_{ax} > 3.75$ m) with a peaked pressure profile [2] , the torus-inward shifted configuration ($R_{ax} < 3.60$ m) [3] and the standard magnetic axis configuration ($R_{ax} = 3.60$ m) with a low magnetic shear. In particular, in low magnetic shear discharges, the frequency of the precursor decreases, and the collapse occurs. This event is called the locked-mode-like instability [4]. In high beta discharges of the LHD, plasma pressure gradient is maintained without the collapse events even if linear MHD analysis predicts the interchange mode is unstable. In a helical plasma, investigating the physical mechanism of the collapse and the relationship between the index of linear MHD instability and the collapse is useful for reflecting MHD stability characteristics of the high beta LHD discharges on the design of a helical fusion plasma.

Two types of locked-mode-like instabilities whose precursors have different radial mode structures are observed in different regimes of a magnetic shear and a beta value of the LHD [4–6]. Regarding the radial profile of internal fluctuations, the precursor of the first type has the odd-type structure respect with the resonant surface. This structure is similar to the tearing mode which is considered to have the large magnetic island (type-I, tearing-type locked-mode-like instability). The other instability has the even-type structure similar to the interchange mode which is considered to not

have the large magnetic island (type-II, interchange-type locked-mode-like instability).

In locked mode discharges of tokamaks [7] and RFPs [8], it is demonstrated that the disruption is escaped by maintaining the rotation of a precursor of the locked mode by using a rotating external RMP [9] and/or tangential NBIs. These results suggest that the slowing-down of the precursor could be related to the trigger mechanism of the collapse.

In the LHD, in order to establish the method of avoiding the collapse, the slowing-down mechanism of the MHD fluctuations due to the locked-mode-like instability has been investigated. From the comparison between the frequency of the precursor and the $\boldsymbol{E} \times \boldsymbol{B}$ flow at the resonant surface during the slowing-down phase, the precursor's frequency is almost the same as the $\boldsymbol{E} \times \boldsymbol{B}$ flow around the resonant surface [5]. It is found that the decrease of the $\boldsymbol{E} \times \boldsymbol{B}$ flow around the resonant surface occurs through the following two stages [5]. The slowing-down of the first stage ($\Delta t_{\mathrm{first}}$) is caused by the movement of the resonant surface to the plasma core region with a small $\boldsymbol{E} \times \boldsymbol{B}$ flow due to increasing the plasma current in the co-direction because the plasma current in the co-direction enhances the increase of the core rotational transform. The slowing-down of the second stage ($\Delta t_{\mathrm{second}}$) occurs by the decrease of the plasma flow around the resonant surface but the resonant surface moves slightly. The above two stages are observed in both of the two types of instabilities [6]. Figure 1 shows the time evolution of (a) amplitude of the magnetic fluctuation due to the m/n = 1/1 mode measured by a magnetic probe, (b) mode frequency, (c) radial magnetic fluctuation amplitude measured by saddle coils, (d) plasma current and (e) the radial profile of an $\boldsymbol{E} \times \boldsymbol{B}$ flow and the radial location of the $\iota/2\pi = 1$ resonant surface in the interchange-type locked-mode-like instability discharge. Here, m and n denote the poloidal and the toroidal mode number, respectively. Furthermore, it is found that the duration time of the slowing-down phase ($\Delta t_{\mathrm{first}} + \Delta t_{\mathrm{second}}$) decreases with the increase of the external RMP (Resonant Magnetic Perturbation) amplitude in interchange-type locked-mode-like discharges [6]. However, the reason for the decrease of an $\boldsymbol{E} \times \boldsymbol{B}$ flow in $\Delta t_{\mathrm{second}}$ is unclear.

On the locked mode of tokamaks, several slowing-down models are proposed [10]. The well-known slowing-down force is the $\boldsymbol{j} \times \boldsymbol{B}$ force. Two types of the $\boldsymbol{j} \times \boldsymbol{B}$ forces are considered depending on what induces $\boldsymbol{B}$: F_{rw} and F_{RMP}. The former is the slowing-down force due to the interaction between the toroidal perturbed current (δj_{t}) due to the instability and the perturbed magnetic field due to the eddy current flowing in the resistive wall of the vacuum vessel. The latter is the force due to the interaction between δj_{t} and the perturbed magnetic field due to the external RMP coils. In the JT-60U tokamak, the relationship between the magnetic fluctuation amplitude and frequency of the precursor during the slowing-down phase is consistent with the prediction of the F_{rw} model, suggesting that the contribution of F_{rw} to the slowing-down is large [11].

In this paper, when an amplitude of the imposed external RMP is changed, the duration time of the slowing-down phase, and the relationship between the magnetic fluctuation amplitude and frequency of the precursor are obtained in locked-mode-like instability with different internal mode structures. The experiment results are compared with the F_{rw} and F_{RMP} models.

This paper is organized as follows. In Sec. 2, the experimental setup is explained. In Sec. 3, the experiment results regarding the locked-mode-like instability are analyzed. In Sec.3.1, the effects of the external RMP on the slowing-down duration time of the interchange-type instability are shown. In Sec. 3.2, the RMP dependence of the slowing-down duration time is compared with the slowing-down models considered in tokamaks. In Sec. 3.3, the experiment results of the tearing-type instability are shown and the effect of the internal structure of the instability on the slowing-down is discussed. In Sec 3.4, the relationship between the magnetic fluctuation amplitude and the frequency of a precursor of both instabilities is shown. The summary and discussion are shown in Sec. 4.

2. Experimental setup

The locked-mode-like instability typically occurs in low magnetic shear plasmas of the LHD. When the plasma aspect ratio A_{p} increases, the magnetic shear in the whole region of a plasma decreases [12]. In this experiment, A_{p} is set to 7.1, which is higher than the configurations with A_{p} = 5.8~6.6, where the reactor-relevant high beta discharges are achieved in the LHD.

For production and heating of plasmas, two tangential NBIs are used. The plasma current increases during discharges due to two tangential NBIs with the same direction and the core rotational transform increases, leading the decrease of the magnetic shear. Perpendicular NBIs are modulated for measurement of an $\boldsymbol{E} \times \boldsymbol{B}$ flow by a charge exchange spectroscopy.

The toroidal and poloidal mode number of magnetic fluctuations are identified by a toroidal array with 6 magnetic probes and a helical array with 15 probes outside a plasma [13]. For evaluation of the amplitude and frequency of a magnetic fluctuation, one of the toroidal array probes located ~ 0.3 m away from the $\iota/2\pi = 1$ surface is used. The slowly changing radial magnetic fluctuation amplitude is measured by two arrays of saddle loops with large cross-section area. The effective area size through which the radial magnetic flux passes is ~ 0.4 m^2. The averaged distance between the saddle loop and the $\iota/2\pi = 1$ surface is ~ 0.5 m.

The definition of $\Delta t_{\mathrm{first}}$ is the duration time when the $\iota/2\pi = 1$ surface largely decreases, and that of $\Delta t_{\mathrm{second}}$ is when the $\iota/2\pi = 1$ surface does not largely change but the $\boldsymbol{E} \times \boldsymbol{B}$ flow velocity

at the $\iota/2\pi$ = 1 surface decreases. Therefore, accurate evaluation of the radial location of the $\iota/2\pi$ = 1 surface is important. During the slowing-down phase in the locked-mode-like instabilities, the small flattering region in the radial electron temperature profile appears due to the m/n = 1/1 precursor. The Thomson scattering system with high spatial resolution can observe the time evaluation of the flattening.

The RMP coil system in the LHD, which has 10 vertical pairs of coils at the top and the bottom, can calibrate the intrinsic error field. According to measurement of the magnetic surface mapping in vacuum [14], there is an m/n = 1/1 magnetic island due to the intrinsic error field, which is almost corrected by the external RMP with RMP coil current (I_{RMP}/B_t) of 110 A/T. Namely, the magnetic island due to the intrinsic error field shrinks to a smaller size. In this paper, I_{RMP}/B_t is changed from 0 to 100 A/T. As I_{RMP}/B_t increases, the corrected error field amplitude decreases, which means that a positive sign of I_{RMP}/B_t corresponds to the opposite phase to the error field. It should be noted that I_{RMP}/B_t and the error field amplitude have a negative correlation.

3. Experiment results

3.1 External RMP effect on interchange-type locked-mode-like instability

Figure 1 shows a typical waveform of the interchange-type locked-mode-like instability discharges where the intrinsic error field is almost cancelled by imposing an external static RMP of I_{RMP}/B_t = 100 A/T. Next, when the amplitude of the imposed external RMP is changed, behaviours of the m/n = 1/1 mode as the precursor are explained. Figure 2 shows typical waveforms with I_{RMP}/B_t of 30 and 15 A/T: (a) (e) radial magnetic fluctuation amplitude measured by saddle loops, (b) (f) mode frequency, (c) (g) magnetic field signal and (d) (h) radial location of the $\iota/2\pi$ = 1. Here, the blue and red hatched regions correspond to the first and second stages of the slowing-down phase, respectively. It should be noted that the timing/amount of gas puffing, the magnetic configuration and the heating condition are almost the same with those in Fig. 1 except for I_{RMP}/B_t. In Figs. 1 and 2, the error field amplitude increases when I_{RMP}/B_t decreases. From Figs. 1 and 2, it is found that Δt_{first} is not largely changed, but Δt_{second} decreases as the error field increases.

Figure 3 shows the external RMP dependence of (a) Δt_{first} and (b) Δt_{second}. Circles display several discharges of the same I_{RMP}/B_t and cross symbols correspond to the averaged value of the discharges of each I_{RMP}/B_t. There is no clear dependence of Δt_{first} on the amplitude of the external RMP in the 0 to 100 A/T region. On the other hand, Δt_{second} decreases as I_{RMP}/B_t decreases. It is found that the external RMP dependence of the duration time of the slowing-down phase ($\Delta t_{slowing} = \Delta t_{first} + \Delta t_{second}$) as reported in ref.[6] reflects the external RMP dependence of Δt_{second}. It is interesting that Δt_{first} for I_{RMP}/B_t = 100 A/T is different from the other cases. The duration time Δt_{first} is determined by the change rate of the current profile and the time when the radial movement of the resonant surface stops. The effect of the external RMP on the change rate and the time as shown in the above is outside the scope of this paper and is a topic for future research.

3.2 Comparison between slowing-down models and experimental observation of locked-mode-like instability

In tokamaks, the slowing-down of the precursor of the locked mode is considered by $\boldsymbol{j} \times \boldsymbol{B}$ forces [10], as shown in section 1. There are two types of $\boldsymbol{j} \times \boldsymbol{B}$ forces, F_{rw} and F_{RMP}, due to a perturbed magnetic field induced by eddy current on resistive wall of a vacuum vessel (B_{eddy}) and by the external coils (B_{RMP}), respectively. Assuming that B_{eddy} is proportional to a perturbed current due to the precursor, δj_t, and its rotation angular frequency ω,

$$F_{rw} \propto \delta j_t^2 \frac{\omega\tau_w}{1+\omega^2\tau_w^2} \sim \delta b_r^2 \frac{\omega\tau_w}{1+\omega^2\tau_w^2}. \quad (1)$$

Here, δj_t is assumed to be proportional to the radial magnetic fluctuation amplitude δb_r measured outside a plasma and τ_w is the wall time constant. Assuming that B_{RMP} is proportional to I_{err}/B_t - I_{RMP}/B_t and the penetration of the external RMP into a plasma is shielded due to the rotation of the external RMP in the frame of the precursor, F_{RMP} is expressed as

$$F_{RMP} \propto \frac{\omega_0'\tau_{rec}}{\sqrt{1+(\omega_0')^2\tau_{rec}^2}} \delta j_t \times (I_{err}/B_t - I_{RMP}/B_t)$$
$$\sim \frac{\omega_0'\tau_{rec}}{\sqrt{1+(\omega_0')^2\tau_{rec}^2}} \delta b_r \times (I_{err}/B_t - I_{RMP}/B_t). \quad (2)$$

Here, I_{RMP}/B_t of 110 A/T corresponds to the compensation coil current for the intrinsic error field, as shown in section 2. In addition, ω_0' is the slip frequency on the external RMP frame and τ_{rec} is the typical reconnection time-scale [10]. In this study, $\omega = \omega_0'$ because the external RMP does not rotate in the laboratory frame.

As mentioned above, δb_r plays an important role on both of F_{rw} and F_{RMP}. Therefore, the dependence of I_{RMP}/B_t on δb_r time-averaged during Δt_{second} of the interchange-type locked-mode-like instability is shown in Figure 4. It is clearly found that δb_r increases with I_{RMP}/B_t in the 0 to 100 A/T region. Note that δb_r is the amplitude of the minor radial component of the magnetic fluctuation due to the m/n =1/1 mode measured by a magnetic probe and the time-averaged value of δb_r during Δt_{second} cannot be evaluated if Δt_{second} = 0.

Figure 5 shows relationships between Δt_{second} and (a) F_{rw} and (b) F_{RMP}. The forces are the time-averaged value during the second stage of the slowing-down phase. When a force strongly contributes to the slowing-down, the slowing-down time decreases with the increase of the force. In other words,

the correlation between the force and the slowing-down time is negative. From Fig.5, $\Delta t_{\mathrm{second}}$ increases with F_{rw}, but $\Delta t_{\mathrm{second}}$ decreases with the increase of F_{RMP}. These results suggest the contribution of F_{RMP} to the slowing-down is large against F_{rw}. Here, τ_{w} is assumed to be 1 ms. Since τ_{w} is the resistive skin time of the vacuum chamber, it is not changed by the instability. If a different value for τ_{w} is selected, the change does not affect the above qualitative behaviour.

3.3 Effect of internal mode structure of locked-mode-like instabilities on slowing-down mechanism

The previous sections show experiment results of the interchange-type locked-mode-like instability. From here, the results of the tearing–type locked-mode-like instability are shown. The tearing-type instability appears in the region of a higher magnetic shear and a lower volume-averaged beta value than the parameter region where the interchange-type instability appears [6]. In order to clarify the slowing-down mechanism of the tearing-type locked-mode-like instability, the external RMP dependences of the slowing-down time of the tearing-type locked-mode-like instability are investigated.

Figure 6 shows the external RMP dependences of $\Delta t_{\mathrm{first}}$ and $\Delta t_{\mathrm{second}}$. Similar to the interchange-type locked-mode-like instability, $\Delta t_{\mathrm{first}}$ of the tearing-type locked-mode-like instability does not depend on $I_{\mathrm{RMP}}/B_{\mathrm{t}}$, but $\Delta t_{\mathrm{second}}$ increases with $I_{\mathrm{RMP}}/B_{\mathrm{t}}$.

Figure 7 shows the dependence of $I_{\mathrm{RMP}}/B_{\mathrm{t}}$ on δb_{r} of the tearing-type locked-mode-like instability, together with the experimental data of the interchange-type instability as already shown in Fig.4. For the tearing-type instability as well as the interchange-type instability, δb_{r} increases with $I_{\mathrm{RMP}}/B_{\mathrm{t}}$. It is interesting that δb_{r} of the interchange-type instability is larger than that of the tearing-type instability at the same $I_{\mathrm{RMP}}/B_{\mathrm{t}}$. The external RMP drives the locked mode in tokamaks, while it suppresses the tearing mode appearing before the mode locking. Similarly, in the locked-mode-like instability discharges, the suppression of the precursor during the slowing-down by the external RMP is also observed. However, the suppression mechanism is a future work.

Figure 8 shows (a) F_{rw} dependence and (b) F_{RMP} dependence of $\Delta t_{\mathrm{second}}$ of the tearing-type locked-mode-like instability together with the interchange-type locked-mode-like instability. Similar to the interchange-type locked-mode-like instability, $\Delta t_{\mathrm{second}}$ increases as F_{rw} increases, but $\Delta t_{\mathrm{second}}$ decreases as F_{RMP} increases. This result suggests that F_{RMP} has a large contribution to the slowing-down regardless of the internal mode structure of the instability, that is, the size of the magnetic island of the instability. However, quantitatively, it can be seen that $\Delta t_{\mathrm{second}}$ of the tearing-type instability is shorter than that of the interchange-type instability at the same F_{RMP}. In order to understand the reason of the quantitative difference, additional data and more systematic analyses are required in future.

3.4 Relationship between amplitude and frequency of precursor during slowing-down phase

Next, the relationship between the frequency (f) and magnetic fluctuation amplitude ($\delta b/B_{\mathrm{t}}$) of the precursor during the slowing-down phase is investigated. According to the JT-60U tokamak's experiment study, the relationship between f and $\delta b/B_{\mathrm{t}}$ of the tearing mode, which is the precursor of the locked mode, is almost consistent with the equation of the F_{rw} model [11]. This result suggests that the contribution of F_{rw} to the slowing-down of the precursor of the locked mode is large. The $\delta b/B_{\mathrm{t}}$-f relationship of the interchange-type instability during the sum of $\Delta t_{\mathrm{first}}$ and $\Delta t_{\mathrm{second}}$ is already reported [6]. However, there was no conclusive result. Here, the $\delta b/B_{\mathrm{t}}$-f relationship only during $\Delta t_{\mathrm{second}}$ is focused upon, and is compared with the relationship based on the following force balance models.

In the force balance model of F_{rw} and a viscous force (F_{vc}), the relationship between the mode frequency and the magnetic fluctuation amplitude of the mode is expressed in [10]. The viscous force is expressed as

$$F_{\mathrm{vc}} \propto (f_0 - f), \tag{3}$$

where f_0 corresponds to the rotation frequency due to the neoclassical flow. The force balance between F_{rw} and F_{vc} is

$$F_{\mathrm{rw}} = -F_{\mathrm{vc}}. \tag{4}$$

Substituting Eqs. (1) and (3) into Eq. (4) yields

$$f = \beta_{\mathrm{rw}}\left(1 + \sqrt{1 - \alpha_{\mathrm{rw}}(\delta b/B_{\mathrm{t}})^2}\right). \tag{5}$$

In addition, the $\delta b/B_{\mathrm{t}}$-f relationship based on the force balance of F_{RMP} and F_{vc} is also derived.

$$F_{\mathrm{RMP}} = -F_{\mathrm{vc}} \tag{6}$$

$$f = -\alpha_{\mathrm{RMP}}(\delta b/B_{\mathrm{t}}) \times (I_{\mathrm{err}}/B_{\mathrm{t}} - I_{\mathrm{RMP}}/B_{\mathrm{t}}) + \beta_{\mathrm{RMP}}. \tag{7}$$

Here, $\omega\tau_{\mathrm{rec}} \gg 1$ is assumed since ω is several krad/s and τ_{rec} ~ 0.2 s in the typical LHD plasma parameters.

On the other hand, if the external RMP is completely penetrated, $F_{\mathrm{RMP,no\text{-}slip}}$ and the $\delta b/B_{\mathrm{t}}$-f relationship based on the $F_{\mathrm{RMP,no\text{-}slip}}$ model is derived as follows[10].

$$F_{\mathrm{RMP,no-slip}} \propto \delta b_{\mathrm{r}} \times (I_{\mathrm{err}}/B_{\mathrm{t}} - I_{\mathrm{RMP}}/B_{\mathrm{t}}). \tag{8}$$

$$f = -\alpha_{\mathrm{RMP,no-slip}}(\delta b/B_{\mathrm{t}}) \times (I_{\mathrm{err}}/B_{\mathrm{t}} - I_{\mathrm{RMP}}/B_{\mathrm{t}}) + \beta_{\mathrm{RMP,no-slip}}. \tag{9}$$

It should be noted that the $\delta b/B_{\mathrm{t}}$-f relationship based on the no-slip model of F_{RMP} has same dependence with that on based on the slip model in the limit of $\omega\tau_{\mathrm{rec}} \gg 1$. Here, α_{rw}, β_{rw}, α_{RMP}, β_{RMP}, $\alpha_{\mathrm{RMP,no\text{-}slip}}$ and $\beta_{\mathrm{RMP,no\text{-}slip}}$ are free parameters. Note that α_{rw}, α_{RMP}, $\alpha_{\mathrm{RMP,no\text{-}slip}}$ (each β) are related with proportionality constant of F_{rw}, F_{RMP} and $F_{\mathrm{RMP,no\text{-}slip}}$ (F_{vc}) except δb and f, respectively.

Figure 9(a) shows the $\delta b/B_{\mathrm{t}}$-f relationship of the interchange-type locked-mode-like instability with the external RMP of $I_{\mathrm{RMP}}/B_{\mathrm{t}}$ = 50 A/T during $\Delta t_{\mathrm{second}}$. Black and grey symbols correspond to the typical behaviour and a

transient behaviour of $\delta b/B_t$ and f, respectively. The transient behaviour is observed for a short time just after the precursor suddenly appears. The intermittent appearance of the precursor is often observed in discharges with external RMP as shown in [6]. The blue dash-dotted lines display the equations of the F_{rw} model with $(\alpha_{rw}, \beta_{rw}) = (1.0 \times 10^8, 0.8)$ and $(2.5 \times 10^7, 0.8)$, and the red dashed line displays the equation of the F_{RMP} model with $(\alpha_{RMP}, \beta_{RMP}) = (6.6 \times 10^1, 1.7)$. The $\delta b/B_t$–f relationship is consistent with F_{RMP}, but it is not consistent with the F_{rw} model. This result suggests that the F_{RMP} model is closer to the experimental data when comparing between the two models.

Figure 9(b) shows the $\delta b/B_t$-f relationship of the tearing-type instability with the external RMP of I_{RMP}/B_t = 50 A/T, which coincides with the F_{RMP} model of $(\alpha_{RMP}, \beta_{RMP}) = (6.6 \times 10^1, 1.4)$. These results suggest that the F_{RMP} model is consistent with the $\delta b/B_t$-f relationship during Δt_{second} of the locked-mode-like instability regardless of the internal mode structure of the instability, supporting the result in section 3.3.

4 Summary and discussion

In order to clarify the slowing-down mechanism of the precursor in the locked-mode-like instability of the LHD, the effect of the external RMP on the slowing-down is investigated. The slowing-down phase can be divided into two stages depending on slowing-down processes. In the first stage of the slowing-down phase, the $\boldsymbol{E} \times \boldsymbol{B}$ flow at the resonant surface decreases due to the movement of the resonance surface to a small $\boldsymbol{E} \times \boldsymbol{B}$ flow region, and in the second stage, the resonance surface is almost constant, but the $\boldsymbol{E} \times \boldsymbol{B}$ flow around the resonant surface itself decreases. This characteristic was already found in the previous research, but it is unclear how the duration time of the second stage is determined. It is investigated how the duration time of the second stage changes by imposing the external RMP, and the RMP dependence of the duration time of the second stage is compared with the slowing-down models for a precursor of the locked mode in tokamaks: F_{rw} and F_{RMP}. The former is the $\boldsymbol{j} \times \boldsymbol{B}$ force by the interaction between a perturbed current due to the instability and a RMP field created by its eddy current, and the latter is the $\boldsymbol{j} \times \boldsymbol{B}$ force by the interaction between the perturbed current and a RMP field due to the external coils at the resonant surface. In addition, F_{RMP} with the complete penetration of the external RMP into the resonant surface ($F_{RMP,no\text{-}slip}$) is also considered.

It is found that the duration time of the second stage decreases as the effective external RMP amplitude increases. The duration time of the second stage has a negative correlation with F_{RMP}, but a positive correlation with F_{rw}. Thus, the above results suggest that F_{RMP} has a large contribution to the slowing-down of the precursor.

Furthermore, the relationship between the magnetic fluctuation amplitude of the precursor and its frequency during the second stage with the external RMP is not consistent with that predicted by the F_{rw} model, but it is consistent with the F_{RMP} model. This result supports the statement that the contribution of F_{RMP} to the slowing-down is larger than F_{rw}.

The above results are on the experiment results of the interchange-type locked-mode-like instability, which has a magnetic island with a small width. The same qualitative results for the tearing-type locked-mode-like instability are obtained. These results suggest that the slowing-down of the precursor is mainly caused by the $\boldsymbol{j} \times \boldsymbol{B}$ force driven by the external RMP regardless of the size of a magnetic island of the instability.

According to an early work, it is reported that the penetration of the external RMP into a plasma is shielded when the external RMP rotates in the frame of the precursor, and that the B_{RMP} is reduced at the resonant surface and F_{RMP} is smaller than that $F_{RMP,no\text{-}slip}$ in the complete penetration case. The Δt_{second} dependence on F_{RMP} shown in Figures 5 (b) and 8 (b) is almost the same against the $F_{RMP,no\text{-}slip}$ in the limit of $\omega\tau_{rec} \gg 1$. The evaluation of experimental B_{RMP} at the resonant surface during the shielding of the penetration of the external RMP is a future research topic.

From the quantitative aspect, the duration time of the second stage of the tearing-type locked-mode-like instability looks shorter than that of the interchange-type instability at the same F_{RMP}. Here, δj_t is assumed to be proportional to δb_r observed outside a plasma. The interchange-type locked-mode instability is expected to have an odd-function-type δj_t profile, which would have larger $|\delta j_t|$ around the resonance surface than in the tearing-type instability for the same δb_r. The improvement of the quantitative accuracy for F_{RMP} of the interchange-type locked-mode-like instability is a future task.

In this study, it is found that the contribution of the electromagnetic force due to the external RMP to the slowing-down of the precursor is large from the dependence of the slowing-down time on the external RMP. On the contrary, even in the discharges with the small external RMP (I_{RMP}/B_t = 100 A/T), the precursor frequency decreases for finite Δt_{second}. According to a previous work of the external RMP effects on the locked-like mode instability, the locked location of the precursor is consistent with the phase of the error field when the finite error field exists. On the other hand, the locked locations of the precursor are not fixed when the error field is almost compensated [15]. The behaviour suggests that the slowing-down mechanism on the precursor of the locked-mode like instability in the case without the error field is different from that with the error field. The slowing-down mechanism in the discharges with the small external RMP should be resolved in future.

Acknowledgements

The authors are grateful to the LHD Operation Group for their excellent technical support. One of the authors (Y.T.)

would like to thank Dr. S.Nishimura (Housei Univ.), Dr. A. Isayama (QST) and Dr. M. Furukawa (Tottori University) for useful discussion. This work was supported in part by NIFS under constract NIFS07KLPH004 and by a dispatch grant from the Future Energy Research Association.

References

[1] Sakakibara S. *et al* 2008 MHD study of the reactor-relevant high-beta regime in the Large Helical Device *Plasma Phys. Control. Fusion* **50** 1–10

[2] Ohdachi S. *et al* 2017 Observation of the ballooning mode thatlimits the operation space of the high-density super-dense- core plasma in the LHD *Nucl. Fusion* **57** 066042

[3] Sakakibara S. *et al* 2002 Effect of MHD activities on pressure profile in high-β plasmas of LHD *Plasma Phys. Control. Fusion* **44** A217–23

[4] Takemura Y. *et al* 2012 Mode locking phenomena observed nearthe stability boundary of the ideal interchange mode of LHD *Nucl. Fusion* **52** 102001

[5] Takemura Y. *et al* 2017 Experimental Study on Slowing-Down Mechanism of Locked-Mode-Like Instability in LHD*Plasma Fusion Res.* **12** 1402028

[6] Takemura Y. *et al* 2019 Study of slowing down mechanism of locked-mode-like instability in helical plasmas *Nucl. Fusion***59** 066036

[7] Snipes J.A., Campbell D.J., Hugon M., Lomas P.J., Nave M.F.F.,Haynes P.S., Hender T.C., Lopes Cardozo N.J. and Schüller F.C. 1988 Large amplitude quasi-stationary MHD modes inJET *Nucl. Fusion* **28** 1085–97

[8] Frassinetti L., Menmuir S., Olofsson K.E.J., Brunsell P.R. and Drake J.R. 2012 Tearing mode velocity braking due to reso- nant magnetic perturbations *Nucl. Fusion* **52** 103014

[9] Okabayashi M. *et al* 2017 Avoidance of tearing mode locking with electro-magnetic torque introduced by feedback-based mode rotation control in DIII-D and RFX-mod *Nucl. Fusion***57** 016035

[10] Fitzpatrick R. 1993 Interaction of tearing modes with external structures in cylindrical geometry (plasma) *Nucl. Fusion* **33**1049–84

[11] Isayama A., Matsunaga G., Ishii Y., Sakamoto Y., Moriyama S., Kamada Y. and Ozeki T. 2010 Effect of magnetic island asso-ciated with neoclassical tearing modes on plasma rotation inJT-60U *Plasma Fusion Res.* **5** 037

[12] Watanabe K.Y., Suzuki Y., Sakakibara S., Yamaguchi T., Narushima Y., Nakamura Y., Ida K., Nakajima N. and Yamada H. 2010 Characteristics of MHD equilibrium and related issues on LHD *Fusion Sci. Technol.* **58** 160–75

[13] Sakakibara S. and Yamada H. (Group LHDE) 2010 Magnetic measurements in LHD *Fusion Sci. Technol.* **58** 471–81

[14] Morisaki T., Shoji M., Masuzaki S., Sakakibara S., Yamada H.and Komori A. 2010 Flux surface mapping in LHD *Fusion Sci. Technol.* **58** 465–70

[15] Sakakibara S. *et al* 2013 Response of MHD stability to reso-nant magnetic perturbation in the Large Helical Device *Nucl.Fusion* **53** 043010

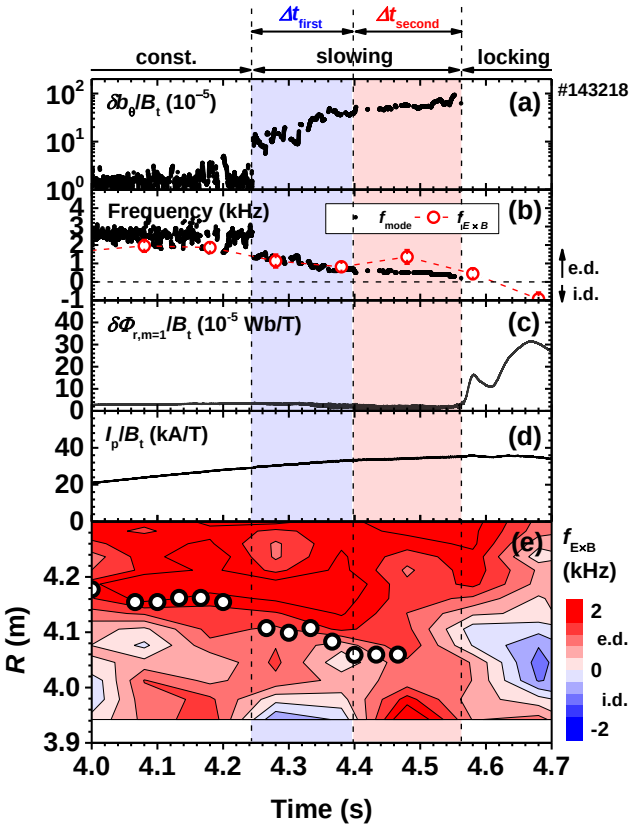

Figure 1. Typical waveform of the interchange-type locked-mode-like instability with I_{RMP}/B_t = 100 A/T. (a) amplitude of a magnetic fluctuation due to the m/n = 1/1 mode measured by a magnetic probe, (b) mode frequency (closed circles) and the $\boldsymbol{E} \times \boldsymbol{B}$ flow at $\iota/2\pi = 1$ (open circles), (c) radial magnetic fluctuation amplitude measured by saddle loops, (d) plasma current, and (e) radial profile of a $\boldsymbol{E} \times \boldsymbol{B}$ flow (contour) and the radial location of $\iota/2\pi = 1$ (open circles). Plus and minus of frequency and red and blue regions of the contour correspond to frequencies in the electron and ion diamagnetic direction, respectively [6].

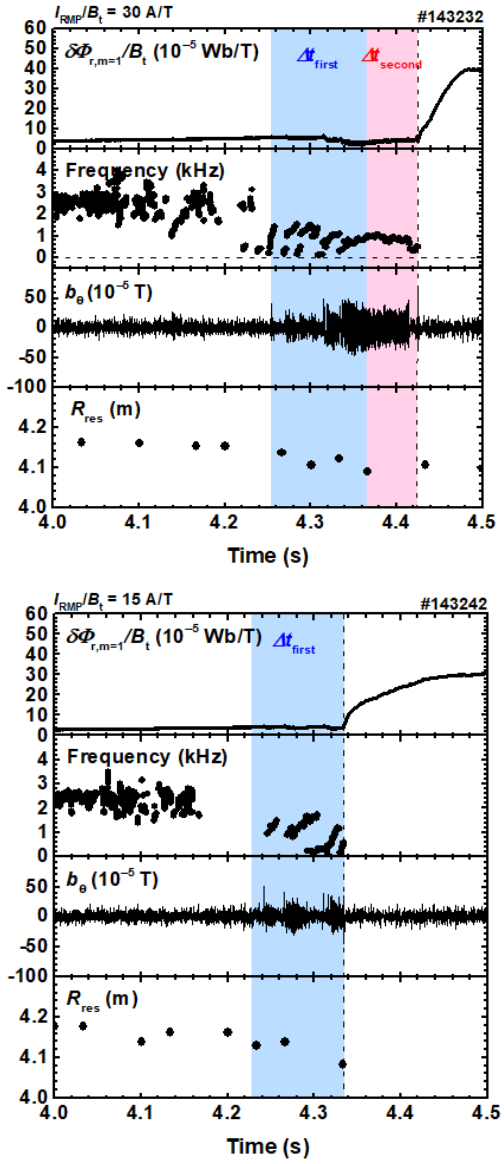

Figure 2. Typical waveform of the interchange-type locked-mode-like instability with (a)-(d) I_{RMP}/B_t = 30 A/T and (e)-(h) 15 A/T. (a) (e) radial magnetic fluctuation amplitude measured by saddle loops, (b) (f) mode frequency, (c) (g) magnetic field signal measured by a magnetic probe, (d) (h) radial location of $\iota/2\pi = 1$. The blue and red hatched regions correspond to the first and second stages of the slowing-down phase, respectively.

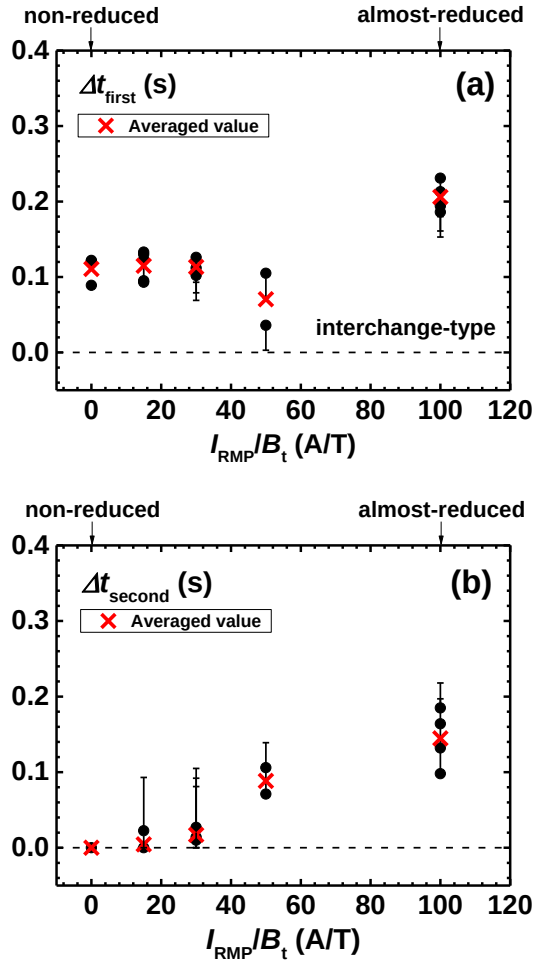

Figure 3. External RMP dependence on (a) $\Delta t_{\mathrm{first}}$ and (b) $\Delta t_{\mathrm{second}}$ of the interchange-type locked-mode-like instability. Cross symbols correspond to the averaged value at each $I_{\mathrm{RMP}}/B_{\mathrm{t}}$.

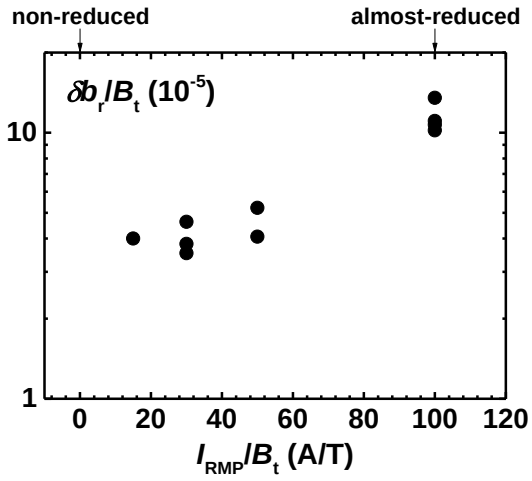

Figure 4. External RMP dependence on the radial magnetic fluctuation amplitude time-averaged during $\Delta t_{\mathrm{second}}$ of the interchange-type locked-mode-like instability.

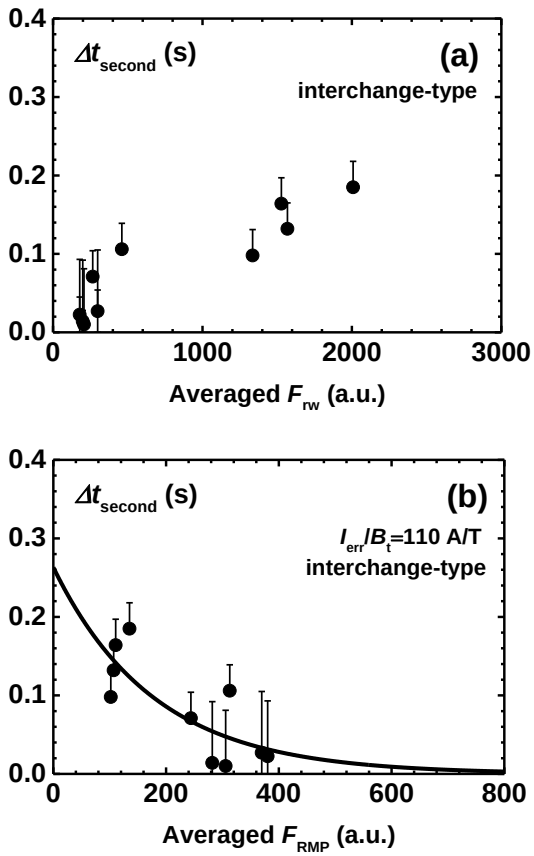

Figure 5. Dependence of (a) F_{rw} and (b) F_{RMP} time-averaged during $\Delta t_{\mathrm{second}}$ on $\Delta t_{\mathrm{second}}$.

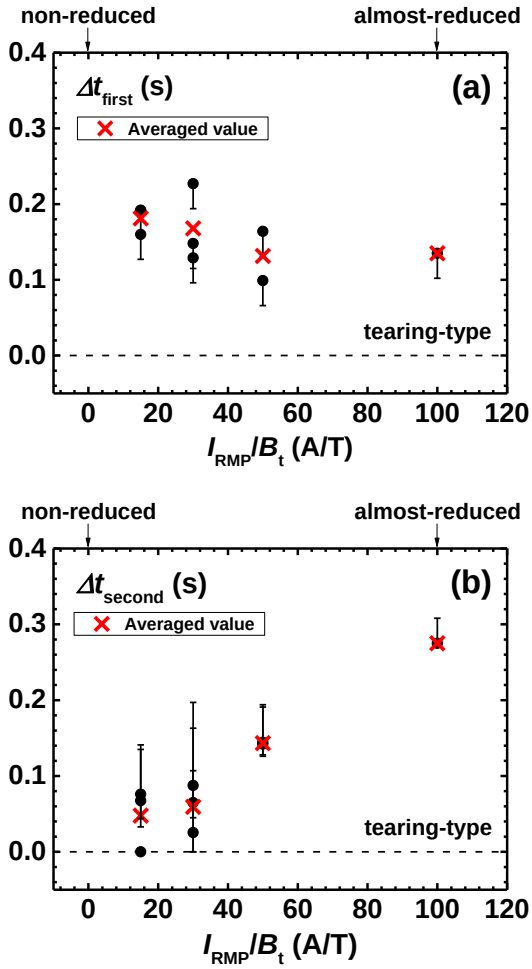

Figure 6. External RMP dependence on (a) $\Delta t_{\mathrm{first}}$ and (b) $\Delta t_{\mathrm{second}}$ of the tearing-type locked-mode-like instability. Cross symbols correspond to the averaged value at each $I_{\mathrm{RMP}}/B_{\mathrm{t}}$.

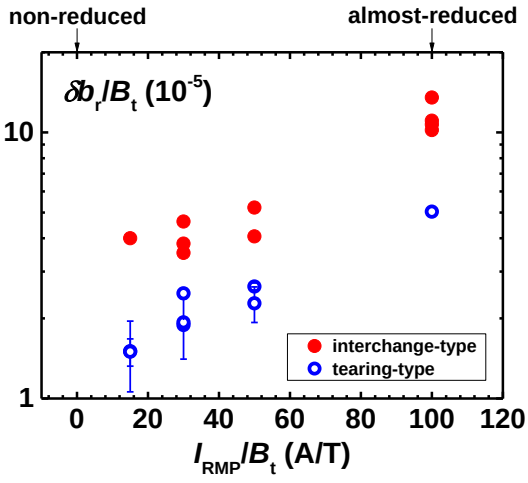

Figure 7. External RMP dependence on the radial magnetic fluctuation amplitude time-averaged during $\Delta t_{\mathrm{second}}$ of the interchange-type and tearing-type locked-mode-like instability.

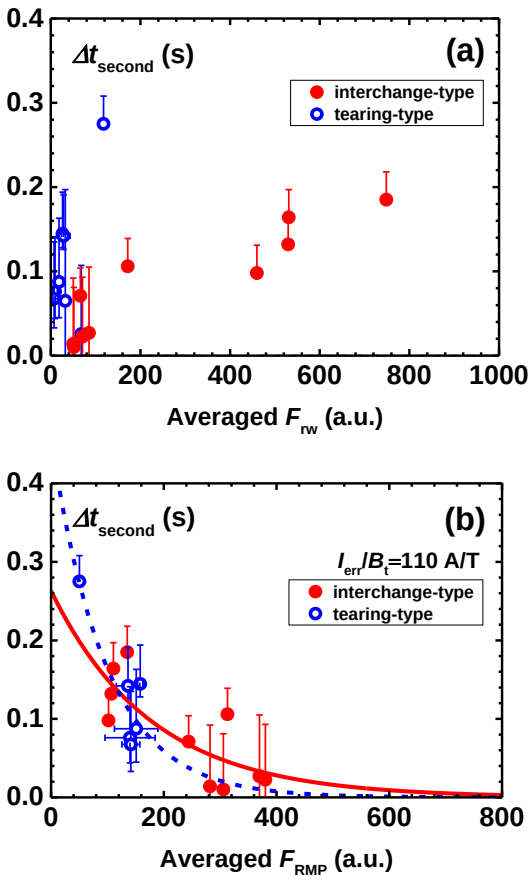

Figure 8. Dependence of (a) F_{rw} and (b) F_{RMP} time-averaged during $\Delta t_{\mathrm{second}}$ on $\Delta t_{\mathrm{second}}$. Here, closed (open) circles correspond to the interchange-type (tearing-type) locked-mode-like instability.

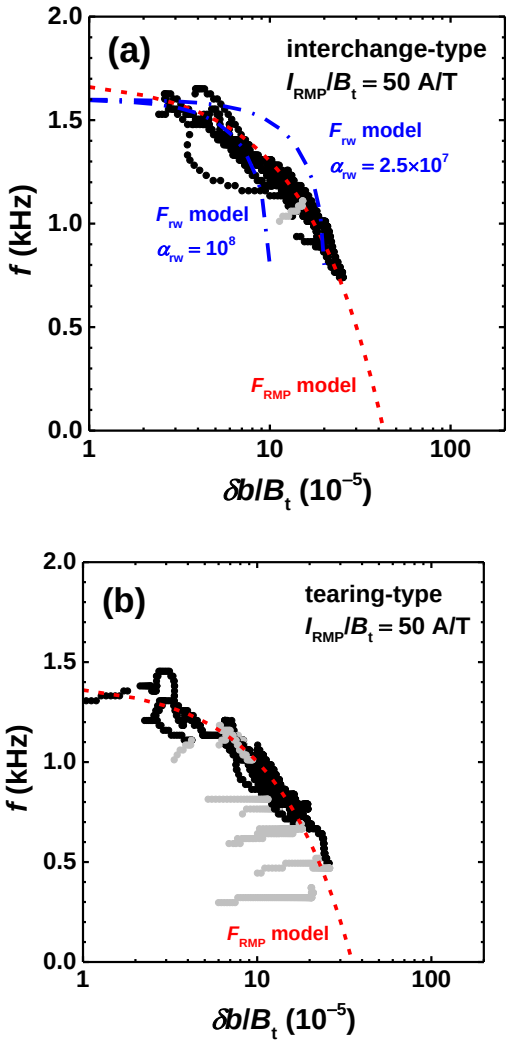

Figure 9. Relationships between the mode frequency and magnetic fluctuation amplitude of (a) the interchange-type and (b) tearing-type locked-mode-like instability during Δt_{second} with an external RMP of the I_{RMP}/B_t = 50 A/T. It should be noted that the magnetic fluctuation amplitude is shown in log scale. Grey symbols indicate data just after the mode suddenly appears. Blue dashed-dotted lines correspond to the equation of the F_{rw} model with different free parameters. Red dashed line corresponds to the equation of the F_{RMP} model.